THE EFFECTS OF SEALING ON THE PLASMA-SPRAYED OXIDE-BASED COATINGS

by Hyung-Jun Kim[1]*, Sidoine Odoul[2], and Young-Gak Kweon[1]

[1]Research Institute of Industrial Science and Technology, Welding Research Center
P.O. Box 135, Pohang, Korea 790-600, khyungj@rist.re.kr
[2]INSA de Lyon, France

ABSTRACT

Electrical insulation and mechanical properties of the plasma sprayed oxide ceramic coatings were studied before and after the sealing treatment of the ceramic coatings. Plasma sprayed Al_2O_3-TiO_2 coating as the reference coating was sealed using three commercial sealants based on polymer. Penetration depth of the sealants to the ceramic coating was evaluated directly from the optical microscope using a fluorescent dye. It is estimated that the penetration depth of the sealants to the ceramic coating is from 0.2 to 0.5 mm depending on the sealants used.

The preliminary test results with a DC puncture tester imply that the dielectric breakdown voltage mechanism of plasma sprayed ceramic coatings has been determined to be a corona mechanism. Dielectric breakdown voltage of the as-sprayed and as-ground samples have shown a linear trend with regard to the thickness, showing an average dielectric strength of 20 kV/mm for the thickness scale studied. It is also shown that grinding the coating before sealing and adding fluorescent dye do not affect the penetration depth of sealants.

All of the microhardness, two-body abrasive wear resistance, bond strength, and surface roughness of the ceramic coating after the sealing treatment are improved. The extent of improvement is different from the sealants used. However, three-point bending stress of the ceramic coating after the sealing treatment is decreased. This is attributed to the reduced micro-crack toughening effect since the cracks propagate easily through the lamellar of the coating without crack deflection and/or branching after the sealing treatment.

KEYWORDS

Plasma spray, oxide ceramic coating, sealing, electrical insulation, mechanical properties

1. Introduction

Plasma sprayed ceramic coatings inevitably contain pores and usually also cracks. Open or closed pores in plasma sprayed coatings can originate from several different factors [1]. These are partially or totally unmelted particles, inadequate flow or fragmentation of the molten particles at impact, shadowing effects due to lower than the optimum angle, and entrapped gas. High cooling rate of the individual splats and poor interlamellar bonding result in vertical and horizontal cracks or voids. These structural defects not only deteriorate the corrosion resistance of the coating-substrate system, but also decrease mechanical properties and consequently the wear resistance of the coatings.

Post-treatment of the plasma sprayed coatings to close the pores and cracks can be performed by several ways [1-4]. These are laser and electron beam surface melting or alloying, hot isostatic pressing (HIP), chemical vapor deposition (CVD), and metal-organic chemical vapor deposition (MOCVD). However, impregnation using polymers, inorganic solutions, or even molten metals is more often performed. Commercially developed sealants are usually based on polymers such as epoxies, phenolics, polyurethanes, silicones, and etc. The purpose of sealing by impregnation is to close or fill open structural defects that are connected to the surface. Thus, the aim of impregnation is to penetrate the coating as great depth as possible.

In most cases, the impregnation is carried out under atmospheric pressure by the methods such as brushing, dipping, or spraying. In this case, the penetration depth of the sealants into the coatings is much less than 100 μm [4-7]. The residual air inside the pores creates a force that opposes to a sealant penetration. It is also reported that bond strength and wear resistance of the coatings are sometimes decreased by impregnation [2,4]. This is attributed to an entrapped air, by-products or solvents evaporated from the sealant, which create the compressive stresses at the substrate-coating interface due to the capillary pressure. If the sealant penetrates and adheres well into the coating but has a high shrinkage at curing, it can create local tensile stress fields causing easier and larger wear-particle detachment.

In this article, commercial sealants based on polymers were studied and electrical insulation and mechanical properties of the coating were tested before and after the impregnation treatment using plasma sprayed alumina-titania coating as the reference coating.

2. Experimental details

The coating samples are composed of three different materials: the substrate (low carbon steel with 5 mm thickness), the bond coat which insures the adhesion of the coating to the substrate, and the ceramic coating.

For this study, the ceramic coating thickness is between 100 μm and 1 mm, and the bond coat is about 100-120 μm. The alumina-titania coating was prepared by conventional plasma spraying with a Sulzer-Metco F4 gun (PT-M1100) and the metallic bond coating was prepared by HVOF (Tafa JP 5000 gun) spraying method for a special application [7].

Three commercially available sealants were investigated. Their properties and curing procedures are listed in Table 1. Sealing was performed in as-sprayed and ground conditions without grinding after the coatings had cooled to room temperature. Coating samples were ultrasonically cleaned and dried at 60°C before sealing treatment. Sealants were prepared just before application and applied by brushing. The "a" and "b" sealants were applied at curing temperature (100°C) in order to decrease the viscosity of the sealants and thus to increase the penetration depth. After the curing, coating samples were ground to eliminate the residue of the sealant left on the surface for further tests.

Table 1. Characteristics and curing conditions of the sealant studied.

Sample code	Brand name	Main component	Applied temp. (oC)	Curing condition	Dielectric strength (volts/mm)	Pentration depth (mm)
a	Metcoseal URS	Urethane	100	100oC/3hrs	10,000	0.2
b	Metcoseal ERS	Epoxy	100	100oC/3hrs	17,600	0.3
c	Dichtol	Ketone	25	100oC/3hrs	-	0.5

The electrical insulation test was conducted with a DC puncture test apparatus according to the ASTM standards D 3755 and D 149 [8-10]. The placement of the electrode on the coating surface and the method of voltage application may greatly influence the results of the tests. Five points per coating sample (50x50 mm) have been measured by a step-by-step method. Dielectric breakdown voltage was obtained from the voltage when the power was automatically shut off in case the current was over 4 mA with increasing voltage. It is also assumed that the electric resistance of steel substrate and metallic bond coat is negligible.

Two-body abrasive wear testing was carried out using a Sugaru wear tester. The details of this wear test are described in References 11 and 12. Buehler grinding papers #120 (grit size of 120 μm) were used for counter abrasives. The load chosen was 3 kg. Each specimen was tested during 2400 revolutions and the data of the first 400 revolutions were discarded to eliminate the roughness effects. The weight was measured up to 0.1 mg every 400 revolutions. The average linear speed was 0.07 m/sec and the total sliding distance was 168 m.

Three-point bending tests were performed to assess the elastic modulus and stress-strain behavior. Samples 5 mm wide and 50 mm long were cut using a diamond saw from thick coatings (2.5 mm) and then the substrate was dissolved using a chemical etch. The testing assembly was mounted on a universal testing machine (model EHF-2B5-102, Simadzu, Inc.), which was interfaced to a recorder for data collection. The crosshead speed was 0.01 mm/sec. The tests were performed on the surface plane in tension. Therefore, the measured direction is the same with the perpendicular direction to the coating surface in the Knoop indentation measurement [13]. Strain gages were attached to the tension face of the coating surface to determine elastic constants and assess stress-strain behavior. The number of tests was three for each specimen.

Bond strength tests of each coating sample were made using a Sebastian IV coating adherence tester (Quad) that is a simple tensile adhesion tester of the thermal sprayed coatings. The maximum strength of epoxy used was 1000 kg/cm^2. The contact area of bonding was 5.7 mm^2, and the epoxy was cured in the dry oven for 70 min. at 150°C. The bond strength of the coating represents the average of at least five measurements.
Porosity (% area) measurements were made using a computer-based image analysis system (Luzex 500) by analyzing 20 fields at a magnification of 200x on each sample. This value represents the total porosity of the coatings. The open porosity was determined with a Mercury Intrusion Porosimeter (MIP, maximum pressure: 410 MPa corresponding to pore size range of 0.003 to 300 μm). The cross-sectional microhardness of the coatings was measured with a conventional Vickers hardness tester under a 500 g load. The average value of 15 measurements was registered as the hardness of the coating sample after discarding the highest and the lowest values.

3. Results and discussion

3-1. Electrical insulation properties of the coatings

Fig. 1 shows the cross sectional optical micrographs of the as-sprayed coating. Ceramic top coating shows a lot of pores and unmelted particles as expected. The total porosity and open porosity in ceramic coating is measured to 8% and 7%, respectively. It is considered that the total porosity is a little bit small because it is measured at a magnification of 200x and thus small pores are hardly detected.

In polarized-microscopy technique [14], two polarizing filters are used. For sealed coating samples, some pores near the surface are filled up by the sealant. The sealed part of the coating presents a more compact structure that allows a partial extinction by using the two crossed polarizing filters. Thus, the observation of the sealed specimens with this technique shows visible contrasts: a bright part where the sealant is absent, and a dark part where it had filled up the pores as can be seen in Fig. 1b. However, the contrast is sometimes not sufficient to measure the penetration depth of the sealants accurately and may greatly depend on the quality of the polishing.

In order to recognize the penetration depth of the sealants to the ceramic top coating, the fluorescent dye (EpoDye) was added when applying the sealants. By adding small amount of EpoDye to the sealant, we can clearly distinguish its penetration. This technique has shown the best reliability for the penetration depth measurements. Fig. 1c shows the different part of the coating: A: residue of the sealant on the coating surface, B: sealed part of the ceramic coating, C: unsealed part of the ceramic coating, D: bond coat.

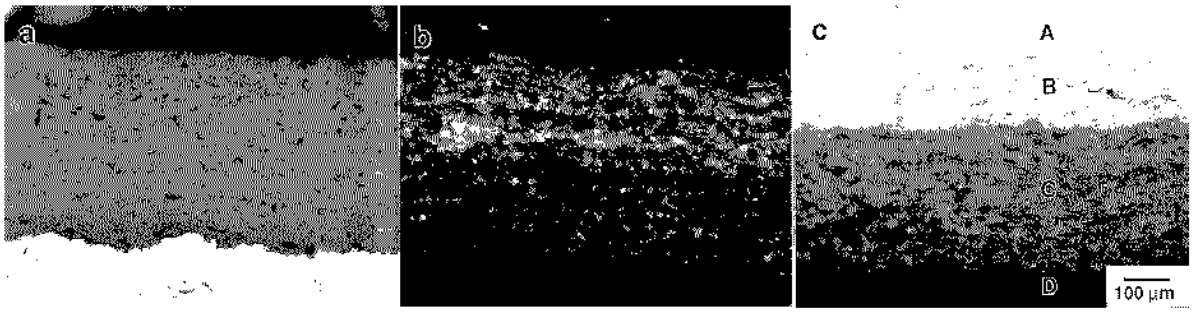

Fig. 1. Cross section of the coating. (a) Conventional optical microscopy. (b) Polarized optical microscopy. (c) Fluorescent light microscopy (A: Residue of the sealant on the coating surface, B: sealed part of the ceramic coating, C: unsealed part of the ceramic coating, D: bond coat)

Fig. 2 shows the results of electrical resistivity measurements of the coatings after ground by #220 emery paper. It is known that general electrical resistivity is the volume resistivity and the surface resistivity depends on the surface state. It is shown that all of the volume resistivity of the coatings are less than those of surface resistivity of the coatings possibly due to anisotrophic structure of the coatings. Volume electrical resistivity of the plasma sprayed 98.5% alumina coating close to that of the bulk alumina (10^{16} Ω cm). It is also shown that electrical resistivity of the coatings is decreased as the TiO_2 content is increased and Cr_2O_2 based coating is the lowest value among investigated.

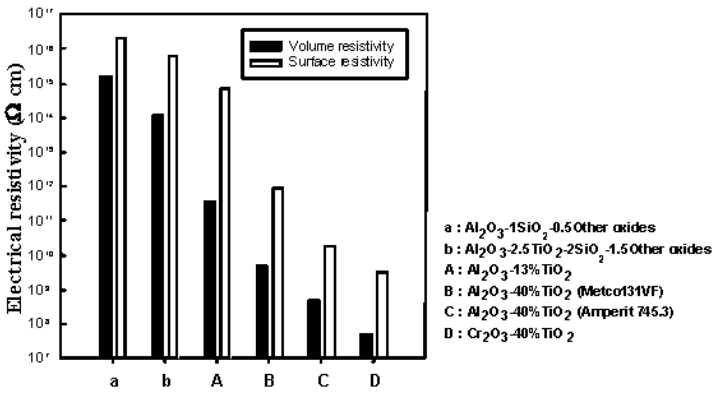

Fig. 2. Electrical resistivity of plasma sprayed ceramic coatings (As-ground, Ceramic coating thickness=0.5 mm).

Fig. 3 shows the results of dielectric breakdown voltage measurements of the coatings after ground by #220 emery paper. Dielectric breakdown voltage of the Al_2O_3-40%TiO_2 coating is around 0.3 kV even though the thickness of the coating approaches 3 mm. Dielectric breakdown voltage of the plasma sprayed Al_2O_3-13%TiO_2 coating increases almost linearly as the thickness of the coatings is increased as expected. Ground samples have similar dielectric strength as compared to the as-sprayed samples if the loss of thickness is taken into account. It has been also shown that grinding the coating before sealing and adding fluorescent dye (EpoDye) do not affect the penetration depth of sealants and the dielectric breakdown voltage of the coatings.

When the breakdown voltage occurs, an electric arc is observed between the electrode and a point of the coating surface. Moreover, two different cases can be distinguished. The electric arc can occur just under the electrode where the electric field is the highest or next to the electrode. Indeed, plasma-sprayed ceramic

coatings are non-homogeneous materials. They may contain dielectric defects of various kinds such as pores and cracks. Thus, dielectric breakdown voltage often occurs in an area of the test specimen other than that where the field intensity is the greatest. Weak spots within volume under stress sometimes determine the test results.

It is concluded that the electrical discharge leads to a physical degradation of the ceramic coating, that is, a complete failure path is formed by chemical decomposition or local erosion [2]. Thus, for a given point, one test is sufficient to definitively damage the coating. Re-testing this point undergoes to a great decrease of the breakdown voltage value that remains constant. This value is controlled by the field intensity that has to be provided to permit an electric arc to occur between the electrode and the path. As a consequence, the breakdown voltage mechanism involved is the corona mechanism, but it may operate in combination with the thermal mechanism.

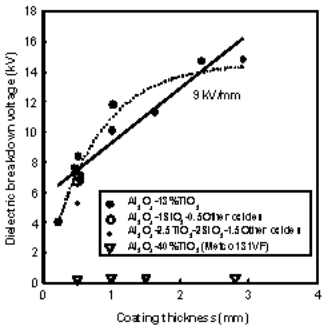

Fig. 3. Dielectric breakdown voltage of plasma sprayed ceramic coatings (As-ground).

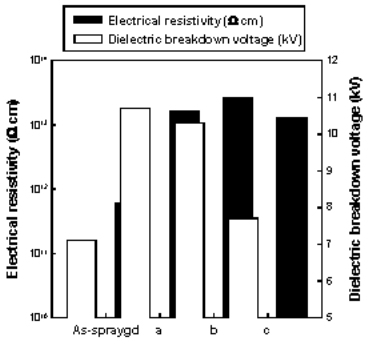

Fig. 4. The effect of sealing treatment on the electrical insulation properties of the coatings.

3-2. Mechanical properties of the coatings

Fig. 5 shows the results of microhardness measurements of the coatings. Microhardness of the coatings was measured at two regions, that is, 50 μm away from the coating surface (noted as Top in Fig. 5) and 50 μm away from the bond coating to ceramic coating (noted as Bottom in Fig. 5). The top hardness represents the as-sealed hardness of the coatings and the bottom hardness represents the unsealed hardness of the coatings except specimen with sealant c. Note that the penetration depth of the specimen with sealant c is almost 500 μm as indicated in Table 1. Bottom hardness of the coatings is about 850 HV except specimen with sealant c. The top hardness of the as-sprayed specimen is just above 600 HV that is well below 850 HV. This is possibly due to more pores at the near surface region. It is clear that the sealing treatment increases the hardness of the coatings.

Fig. 6 shows the results of wear and bond strength tests of the coatings. It is also clear that sealing treatment increases both the wear resistance and the bond strength of the coatings. Although penetration depth of the specimen with sealant c is the largest (500 μm), the improvement of the wear resistance and the bond strength of the coatings is the smallest compared to specimens with sealants a and b. It is noted that wear tests of the coatings were conducted within sealed part of the coatings and thus wear rate of the coatings corresponds to only the sealing effect of the coatings.

It is considered that sealing treatment gives adhesive effect along the lamellar of the coatings resulting in improvement of the wear resistance and the bond strength of the coatings. It means that the sealed coating needs more stress to detach each lamellar of the ceramic coating. It is also noted that the failure of the coating after the bond strength test has always occurred within the ceramic coating. It is estimated that the penetration depth of the sealant b to the ceramic coating is about 300 μm from the cross sectional micrograph. This indirect estimation of the penetration depth of the sealant to the ceramic coating coincides with the direct measurement of the penetration depth of the sealant as shown in Fig. 1c.

Table 2 summarizes the results of three-point bending tests. The elastic modulus of a coating can be obtained as the tangent of the stress-strain curve of that coating. The modulus of a coating changes with stress increase because of the nonlinear stress-strain curve of the coating. It is expected that the elastic modulus values measured by three-point bending tests are significantly low compared to those measured by the Knoop indentation test and around 6-21 GPa, irrespective of coating compositions [13]. These results are consistent with the works of Leigh, et al [15] and Shi, et al [16]. Their results are that the elastic modulus values determined by four-point bend test for plasma-sprayed zirconia and alumina are 19-41 GPa depending on porosity (9-12%) and 12.3 GPa, respectively.

Surprisingly, all of the 0.2% yield strain (ε_Y), 0.2% yield stress (σ_Y), elastic modulus, fracture strain (ε_f),

and fracture stress (σ_f) values show a decreasing tendency from the as-sprayed coating to the sealed coatings although sealed thickness (less than 0.5 mm) of the coatings are less than 25% of whole specimen tested (2.5 mm). Lower value of elastic modulus for sealed specimens is understandable because main components of the sealants are based on polymers that have very low values of elastic modulus.

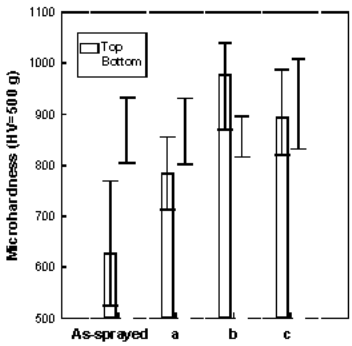

Fig. 5. The effect of sealing treatment on the hardness of the coating

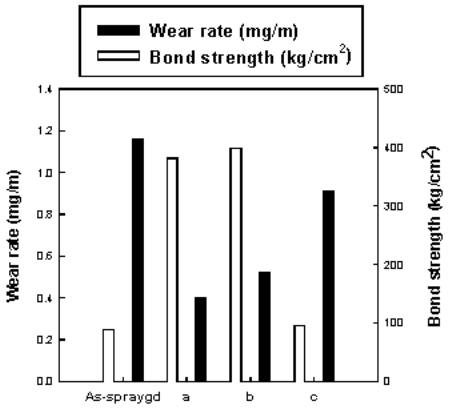

Fig. 6. The effects of sealing treatment on the wear rate and bond strength of the coating.

Non-linear stress-strain behavior of the coatings correlates with their microstructures. Inelastic strain results from microcracks, pores, and lamellar structure. The level of inelastic strain depends on the strain needed for microcrack extension and crack deflection and branching before catastrophic failure [17]. This is a microcrack toughening effect due to the lamellar structure of the coating since the plasma-sprayed materials can be considered as a collection of weakly bonded tiles. This is also called pseudo-ductility that is due to the cracks opening up [18]. It seems that the sealants fill in microcracks and pores resulting in reducing the ductility of the coatings. Thus, sealed coatings exhibit reduced values of elastic stress and strain, and fracture stress and strain caused by reduced toughening effects since the cracks propagate easily through the lamellar of the coating without crack deflection and/or branching after the sealing treatment.

Table 2. Summary of 3-point bending test results.

Specimen code	ε_y (%)	σ_y (kg/mm2)	E (GPa)	ε_f (%)	σ_f (kg/mm2)
A	0.8	10.8	14.0	1.7	18.0
A-a	0.7	9.5	13.6	1.5	14.9
A-b	0.6	8.5	13.5	1.1	11.6
A-c	0.7	8.9	12.4	1.3	13.0

* ε_y, σ_y : 0.2% offset

4. Conclusions

Electrical insulation and mechanical properties of the plasma sprayed ceramic coating were studied before and after the sealing treatment of the ceramic coating. Plasma sprayed Al_2O_3-TiO_2 coating as the reference coating was sealed using three commercial sealants based on polymer. Penetration depth of the sealants to the ceramic coating was evaluated directly from the optical microscope using a fluorescent dye. It is estimated that the penetration depth of the sealants to the ceramic coating is from 0.2 to 0.5 mm depending on the sealants used.

It is shown that the breakdown voltage mechanism of plasma-sprayed alumina coatings has been determined as a corona mechanism partly combined with the thermal mechanism. Ground samples have similar dielectric strength as compared to the as-sprayed samples if the loss of thickness is taken into account. Dielectric breakdown voltage of the as-sprayed and as-ground samples of the APS sprayed Al_2O_3-13%TiO_2 have shown a linear trend with regard to the thickness. It has been shown that grinding the coating before sealing

and adding fluorescent dye (EpoDye) do not affect the penetration depth of sealants. Although the penetration of sealant to the ceramic coating have reached 300 μm, it has not been clearly established the effects of curing time and temperature.

All of the microhardness, two-body abrasive wear resistance, bond strength, and surface roughness of the ceramic coating after the sealing treatment are improved. The extent of improvement is different from the sealants used. However, three-point bending stress of the ceramic coating after the sealing treatment is decreased. This is attributed to the reduced micro-crack toughening effect since the cracks propagate easily through the lamellar of the coating without crack deflection and/or branching after the sealing treatment.

References

[1] R.B. Heimann, *Plasma-Spray Coating, Principle and Application*, VCH, 1996, p.164-165.
[2] J. Knuuttila, P. Sorsa, and T. Mantyla, J. of Thermal Spray Technology, **8** (1999), 249-257.
[3] L. Pawlowski, *The Science and Engineering of Thermal Spray Coatings*, John Wiley & Sons, 1995, p.64-66.
[4] E. Lugscheider, P. Jokiel, V. Messerschmidt, and G. Beckschulte, Surface Engineering, **10** (1994), 46-51.
[5] B. Wielage, U. Hofmann, S. Steinhauser, and G. Zimmermann, Surface Engineering, **14** (1998), 136-138.
[6] B. Wielage, U. Hofmann, S. Steinhauser, and G. Zimmermann, *Surface Modification Technologies XI*, Edited by T.S. Sudarshan, M. Jeandin, and K.A. Khor, The Institute of Materials, London, 1998, p.328-335.
[7] H.J. Kim, RIST research project No. 99M033, 2000.
[8] Standard test method for dielectric breakdown voltage and dielectric strength of solid electrical insulating materials under direct-voltage stress, ASTM D 3755.
[9] Standard test method for dielectric breakdown voltage and dielectric strength of solid electrical insulating materials at commercial power frequencies, ASTM D 149
[10] Standard terminology relating to electrical insulation, ASTM D 1711
[11] S. Kumar, D.P. Mondal, H.K. Khaira, and A.K. Jha, J. of Mater. Engineering and Performance, **8** (1999), 711-715.
[12] A.K. Jha, B.K. Prasan, R. Dasgupta, and O.P. Modi, J. of Mater. Engineering and Performance, **8** (1999), 190-196.
[13] H.J. Kim and Y.G. Kweon, Thin Solid Films, **342** (1999), 202-207.
[14] Metallography and Microstructures, Metals Handbook Ninth edition, vol. 9, p.76-78.
[15] S.H. Leigh, C.C. Berndt, S. Sampath, and H. Herman, *Proc. of the 9th National Thermal Spray Conf.*, Cincinnati, Ohio, USA, 7-11 October, 1996, p.835-840.
[16] K.S. Shi, Z.Y. Qian, and M.S. Zhuang, J. Am. Ceram. Soc., **71** (1988), 924-929..
[17] C.K. Lin, S.H. Leigh, C.C. Berndt, R.V. Gansert, S. Sampath, and H. Herman, Acoustic emission responses of plasma sprayed ceramics during four point bend tests, *Ceramic Eng. and Sci. Proc.*, 1996, p.44-50.
[18] P.A. Siemers and R.L. Mehan, Mechanical physical properties of plasma-sprayed stabilized zirconia, *Ceramic Eng. and Sci. Proc.*, 1983, p.828-840.